Supplementary Information

For

Quantum Mechanical and Classical Calculation of the Transport and Relaxation Properties of He...CO_2 Complex Using a New PES

Ebrahim Nemati-Kande, [a*] Fatemeh Aghababaei, [a] Salar Sadeghi, [a]

[a] *Department of Physical Chemistry, Chemistry Faculty, Urmia University, Urmia, Iran*

*Corresponding author.

E-mail address: e.nemati@urmia.ac.ir

Table S.1. The SBE transport and relaxation properties at different temperatures for even paritiy of He…CO_2 complex.

T (K)	$\mathfrak{S}^{(1)}_D$	$\mathfrak{S}^{(2)}_\eta$	$\mathfrak{S}_T$	$\mathfrak{S}_{DPR}$	$\mathfrak{S}_{prod}$	$\mathfrak{S}_{ROT}$	D_{12}(cm^2.s^{-1})	η_{12}(μPa.s)
25	12.173	0.747	25.173	36.928	0.228	48.196	0.006	1.691
50	8.672	0.533	14.207	22.615	0.151	29.308	0.025	3.354
75	7.462	0.457	10.618	17.569	0.122	22.428	0.054	4.790
100	6.856	0.419	8.864	14.985	0.107	18.856	0.091	6.032
125	6.485	0.396	7.823	13.406	0.097	16.658	0.134	7.138
150	6.229	0.380	7.122	12.332	0.090	15.149	0.183	8.146
175	6.038	0.368	6.608	11.547	0.085	14.033	0.238	9.081
200	5.888	0.359	6.209	10.941	0.080	13.162	0.298	9.958
225	5.767	0.351	5.885	10.454	0.077	12.455	0.364	10.789
250	5.664	0.345	5.614	10.049	0.073	11.863	0.434	11.583
275	5.576	0.339	5.381	9.704	0.071	11.356	0.508	12.346
300	5.499	0.334	5.177	9.405	0.068	10.913	0.587	13.083
325	5.430	0.330	4.995	9.141	0.066	10.521	0.670	13.797
350	5.368	0.326	4.831	8.905	0.064	10.170	0.758	14.491
375	5.311	0.323	4.679	8.692	0.062	9.855	0.849	15.168
400	5.258	0.319	4.539	8.499	0.060	9.568	0.945	15.829
425	5.209	0.316	4.407	8.321	0.058	9.307	1.045	16.475
450	5.163	0.313	4.281	8.157	0.056	9.068	1.149	17.108
475	5.119	0.311	4.161	8.005	0.055	8.848	1.256	17.728
500	5.077	0.308	4.046	7.864	0.053	8.645	1.368	18.337
525	5.037	0.306	3.935	7.733	0.052	8.457	1.484	18.935
550	4.999	0.303	3.827	7.609	0.051	8.283	1.603	19.524
575	4.962	0.301	3.722	7.493	0.049	8.121	1.726	20.102
600	4.926	0.299	3.620	7.384	0.048	7.970	1.854	20.672
625	4.891	0.297	3.521	7.282	0.047	7.829	1.985	21.233
650	4.857	0.296	3.425	7.185	0.046	7.697	2.120	21.786
675	4.824	0.294	3.331	7.093	0.045	7.573	2.259	22.332
700	4.791	0.292	3.240	7.005	0.044	7.457	2.402	22.871
725	4.759	0.291	3.152	6.923	0.043	7.348	2.548	23.403
750	4.727	0.289	3.065	6.844	0.042	7.245	2.699	23.928
775	4.696	0.288	2.982	6.769	0.041	7.148	2.854	24.448
800	4.666	0.286	2.900	6.698	0.040	7.056	3.013	24.962
825	4.636	0.285	2.822	6.630	0.040	6.969	3.175	25.471
850	4.606	0.284	2.745	6.564	0.039	6.887	3.342	25.974
875	4.577	0.282	2.671	6.502	0.038	6.809	3.513	26.474
900	4.547	0.281	2.599	6.443	0.037	6.735	3.689	26.970
925	4.518	0.280	2.529	6.385	0.037	6.664	3.868	27.461
950	4.490	0.279	2.462	6.331	0.036	6.597	4.052	27.950
975	4.461	0.277	2.396	6.278	0.035	6.532	4.239	28.436
1000	4.433	0.276	2.333	6.228	0.035	6.471	4.432	28.920
1025	4.405	0.275	2.272	6.179	0.034	6.411	4.628	29.402
1050	4.377	0.274	2.212	6.133	0.034	6.354	4.829	29.884
1075	4.349	0.273	2.155	6.088	0.033	6.299	5.035	30.364
1100	4.321	0.272	2.099	6.044	0.032	6.246	5.245	30.845
1125	4.293	0.270	2.045	6.002	0.032	6.194	5.460	31.326
1150	4.266	0.269	1.993	5.962	0.031	6.143	5.680	31.808
1175	4.238	0.268	1.943	5.923	0.031	6.094	5.904	32.292
1200	4.210	0.267	1.894	5.885	0.030	6.046	6.134	32.778
1225	4.183	0.266	1.846	5.849	0.030	5.999	6.368	33.268
1250	4.155	0.265	1.801	5.813	0.029	5.952	6.607	33.761
1275	4.128	0.263	1.756	5.779	0.029	5.907	6.852	34.259
1300	4.100	0.262	1.713	5.746	0.028	5.861	7.102	34.761
1325	4.073	0.261	1.671	5.713	0.028	5.816	7.357	35.270
1350	4.045	0.259	1.631	5.682	0.028	5.772	7.618	35.784
1375	4.017	0.258	1.592	5.651	0.027	5.727	7.885	36.305
1400	3.990	0.257	1.554	5.621	0.027	5.683	8.157	36.834
1425	3.962	0.255	1.517	5.592	0.026	5.639	8.435	37.371
1450	3.934	0.254	1.481	5.564	0.026	5.595	8.719	37.916
1475	3.906	0.252	1.446	5.536	0.026	5.550	9.010	38.471
1500	3.878	0.251	1.413	5.508	0.025	5.506	9.306	39.036

Table S.2. The SBE transport and relaxation properties at different temperatures for odd parity of He…CO_2 complex.

T (K)	$\mathfrak{S}^{(1)}_D$	$\mathfrak{S}^{(2)}_\eta$	$\mathfrak{S}_T$	$\mathfrak{S}_{DPR}$	$\mathfrak{S}_{prod}$	$\mathfrak{S}_{ROT}$	D_{12}(cm^2.s^{-1})	η_{12}(μPa.s)
25	12.164	0.747	25.149	36.681	0.226	48.205	0.006	1.691
50	8.669	0.533	14.181	22.253	0.151	29.285	0.025	3.354
75	7.460	0.457	10.622	17.281	0.122	22.436	0.054	4.790
100	6.854	0.419	8.877	14.758	0.107	18.873	0.091	6.033
125	6.483	0.396	7.837	13.221	0.097	16.675	0.134	7.139
150	6.227	0.380	7.133	12.177	0.090	15.164	0.183	8.147
175	6.037	0.368	6.617	11.414	0.085	14.046	0.238	9.081
200	5.888	0.359	6.216	10.824	0.080	13.174	0.298	9.958
225	5.766	0.351	5.891	10.350	0.077	12.467	0.364	10.789
250	5.664	0.345	5.619	9.955	0.073	11.874	0.434	11.583
275	5.576	0.339	5.385	9.619	0.070	11.366	0.508	12.346
300	5.500	0.334	5.181	9.327	0.068	10.922	0.587	13.083
325	5.431	0.330	4.999	9.069	0.066	10.530	0.670	13.797
350	5.369	0.326	4.834	8.838	0.063	10.179	0.758	14.491
375	5.312	0.323	4.682	8.630	0.061	9.863	0.849	15.168
400	5.259	0.319	4.541	8.440	0.060	9.576	0.945	15.828
425	5.210	0.316	4.408	8.266	0.058	9.314	1.045	16.474
450	5.164	0.313	4.282	8.105	0.056	9.073	1.148	17.107
475	5.120	0.311	4.162	7.956	0.055	8.852	1.256	17.728
500	5.078	0.308	4.046	7.817	0.053	8.648	1.368	18.337
525	5.038	0.306	3.934	7.688	0.052	8.459	1.483	18.935
550	5.000	0.303	3.825	7.566	0.050	8.284	1.603	19.523
575	4.963	0.301	3.720	7.452	0.049	8.121	1.726	20.102
600	4.927	0.299	3.618	7.345	0.048	7.969	1.853	20.672
625	4.892	0.297	3.519	7.243	0.047	7.827	1.984	21.234
650	4.857	0.296	3.422	7.147	0.046	7.693	2.119	21.788
675	4.824	0.294	3.328	7.057	0.045	7.569	2.258	22.334
700	4.791	0.292	3.236	6.970	0.044	7.452	2.401	22.873
725	4.759	0.291	3.147	6.888	0.043	7.342	2.548	23.406
750	4.727	0.289	3.061	6.811	0.042	7.238	2.699	23.932
775	4.696	0.288	2.977	6.736	0.041	7.140	2.854	24.453
800	4.665	0.286	2.895	6.665	0.040	7.047	3.013	24.968
825	4.635	0.285	2.816	6.598	0.039	6.960	3.176	25.478
850	4.604	0.283	2.739	6.533	0.039	6.877	3.344	25.983
875	4.575	0.282	2.665	6.471	0.038	6.798	3.515	26.484
900	4.545	0.281	2.593	6.412	0.037	6.724	3.690	26.981
925	4.516	0.280	2.523	6.355	0.036	6.652	3.870	27.475
950	4.487	0.278	2.456	6.301	0.036	6.584	4.054	27.965
975	4.458	0.277	2.390	6.248	0.035	6.519	4.243	28.453
1000	4.429	0.276	2.327	6.198	0.034	6.457	4.435	28.939
1025	4.401	0.275	2.265	6.150	0.034	6.397	4.633	29.423
1050	4.372	0.274	2.206	6.103	0.033	6.339	4.834	29.906
1075	4.344	0.273	2.149	6.058	0.033	6.284	5.041	30.389
1100	4.316	0.271	2.093	6.015	0.032	6.230	5.252	30.872
1125	4.287	0.270	2.039	5.974	0.032	6.178	5.468	31.355
1150	4.259	0.269	1.987	5.933	0.031	6.127	5.688	31.840
1175	4.231	0.268	1.937	5.894	0.030	6.077	5.914	32.326
1200	4.203	0.267	1.888	5.857	0.030	6.029	6.144	32.815
1225	4.175	0.265	1.841	5.820	0.030	5.981	6.379	33.307
1250	4.147	0.264	1.795	5.785	0.029	5.935	6.620	33.803
1275	4.119	0.263	1.750	5.750	0.029	5.889	6.866	34.304
1300	4.091	0.262	1.707	5.717	0.028	5.843	7.117	34.809
1325	4.063	0.260	1.666	5.685	0.028	5.798	7.374	35.320
1350	4.035	0.259	1.625	5.653	0.027	5.753	7.637	35.838
1375	4.007	0.258	1.586	5.623	0.027	5.708	7.905	36.362
1400	3.979	0.256	1.548	5.593	0.026	5.664	8.179	36.894
1425	3.951	0.255	1.512	5.564	0.026	5.620	8.459	37.434
1450	3.922	0.253	1.476	5.535	0.026	5.575	8.745	37.982
1475	3.894	0.252	1.441	5.507	0.025	5.531	9.037	38.541
1500	3.866	0.250	1.408	5.480	0.025	5.486	9.336	39.108

Table S.3. Calculated interaction viscosity coefficient (η_{12}) for He…CO_2 complex at different temperatures, using the Mason-Monchick approximation (MMA) and Boltzmann weighting method (BWM).

	η_{12}(μPa.s)			η_{12}(μPa.s)			η_{12}(μPa.s)	
T(K)	BWM	MMA	T(K)	BWM	MMA	T(K)	BWM	MMA
50	3.150	3.072	600	18.894	18.830	1300	30.549	30.511
75	4.480	4.389	625	19.383	19.321	1350	31.269	31.232
100	5.648	5.550	650	19.864	19.804	1400	31.979	31.942
125	6.688	6.586	675	20.338	20.279	1450	32.678	32.643
150	7.631	7.529	700	20.805	20.747	1500	33.368	33.334
175	8.500	8.400	725	21.266	21.209	1550	34.049	34.015
200	9.312	9.214	750	21.720	21.665	1600	34.722	34.688
225	10.078	9.983	775	22.168	22.114	1650	35.385	35.353
250	10.805	10.713	800	22.611	22.557	1700	36.041	36.010
275	11.501	11.411	825	23.048	22.996	1750	36.690	36.659
300	12.169	12.082	850	23.480	23.428	1800	37.331	37.300
325	12.814	12.729	875	23.907	23.856	1850	37.964	37.935
350	13.438	13.356	900	24.329	24.279	1900	38.591	38.563
375	14.043	13.963	925	24.746	24.697	1950	39.212	39.184
400	14.632	14.554	950	25.159	25.111	2000	39.826	39.798
425	15.206	15.130	975	25.568	25.521	2100	41.036	41.010
450	15.766	15.692	1000	25.973	25.926	2200	42.223	42.198
475	16.313	16.242	1050	26.770	26.725	2300	43.389	43.365
500	16.849	16.780	1100	27.552	27.509	2400	44.535	44.511
525	17.375	17.307	1150	28.320	28.278	2500	45.661	45.638
550	17.890	17.824	1200	29.076	29.035			
575	18.396	18.332	1250	29.818	29.779			

Table S.4. Calculated interaction diffusion coefficient (D_{12}) for He…CO_2 complex at different temperatures, using the Mason-Monchick approximation (MMA) and Boltzmann weighting method (BWM).

	$D_{12}(cm^2.s^{-1})$			$D_{12}(cm^2.s^{-1})$			$D_{12}(cm^2.s^{-1})$	
T(K)	BWM	MMA	T(K)	BWM	MMA	T(K)	BWM	MMA
50	0.023	0.023	600	1.659	1.655	1300	5.797	5.792
75	0.049	0.048	625	1.773	1.768	1350	6.161	6.155
100	0.083	0.081	650	1.890	1.885	1400	6.532	6.527
125	0.122	0.120	675	2.009	2.004	1450	6.912	6.906
150	0.167	0.165	700	2.131	2.127	1500	7.299	7.294
175	0.217	0.215	725	2.256	2.251	1550	7.694	7.689
200	0.272	0.269	750	2.383	2.379	1600	8.097	8.092
225	0.331	0.328	775	2.514	2.509	1650	8.508	8.502
250	0.394	0.391	800	2.646	2.641	1700	8.926	8.920
275	0.462	0.459	825	2.781	2.777	1750	9.351	9.346
300	0.533	0.530	850	2.919	2.914	1800	9.784	9.778
325	0.609	0.605	875	3.059	3.054	1850	10.224	10.218
350	0.688	0.684	900	3.202	3.197	1900	10.671	10.665
375	0.770	0.766	925	3.347	3.342	1950	11.125	11.119
400	0.856	0.852	950	3.495	3.490	2000	11.585	11.580
425	0.945	0.942	975	3.644	3.639	2100	12.528	12.523
450	1.038	1.034	1000	3.797	3.792	2200	13.497	13.492
475	1.134	1.130	1050	4.108	4.103	2300	14.493	14.488
500	1.233	1.229	1100	4.428	4.423	2400	15.515	15.509
525	1.335	1.331	1150	4.758	4.752	2500	16.561	16.556
550	1.440	1.436	1200	5.096	5.090			
575	1.548	1.544	1250	5.442	5.437			

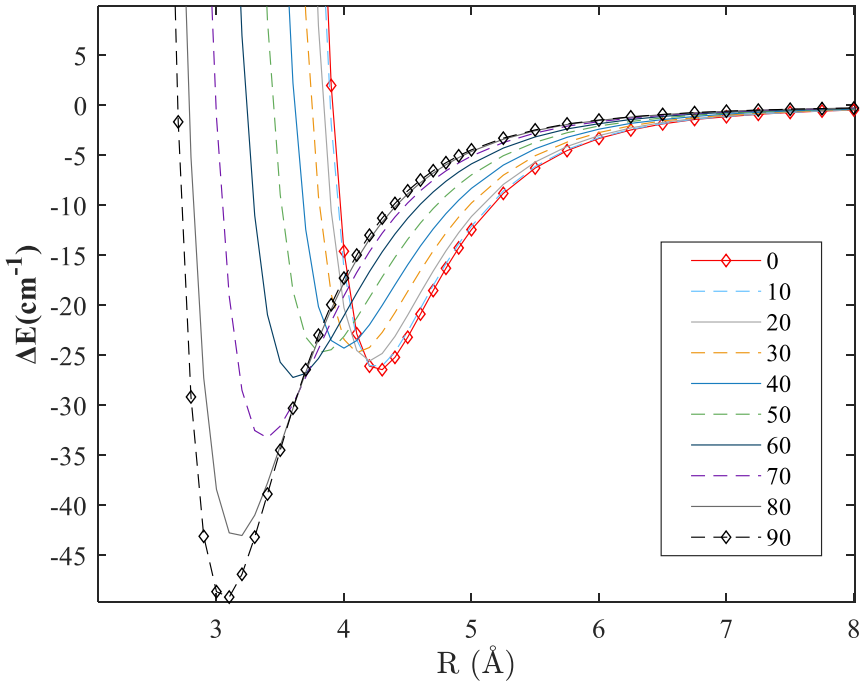

Fig. S.1. Calculated potentials for He…CO_2 complex at θ = 0°- 90° as function of separation (R) between the CO_2 center of mass and He atom using RCCSD(T)/aQz-BF method.

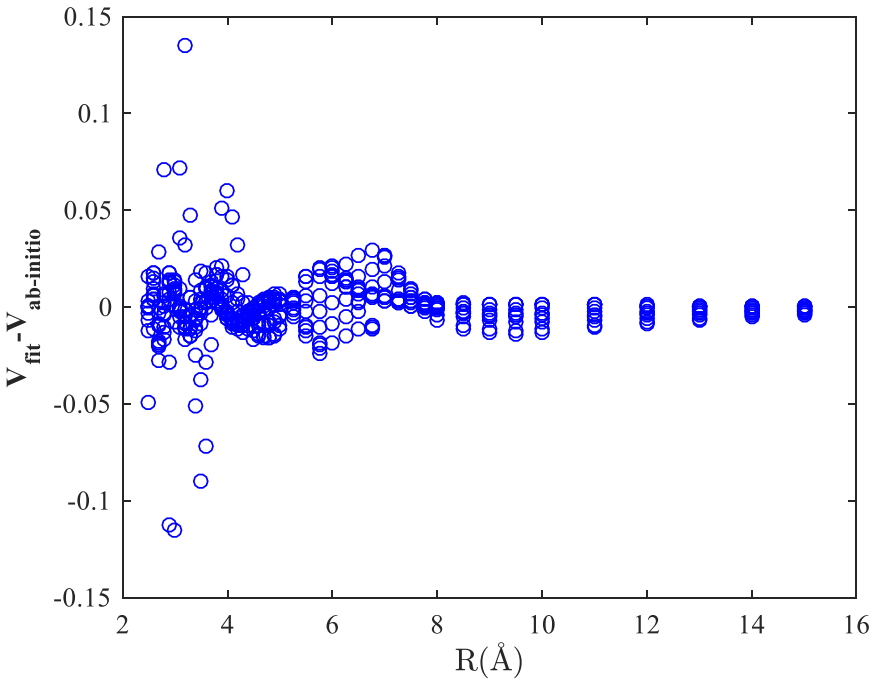

Fig. S.2. Deviation of the ab-initio potentials and fitted values for He…CO_2 PES.

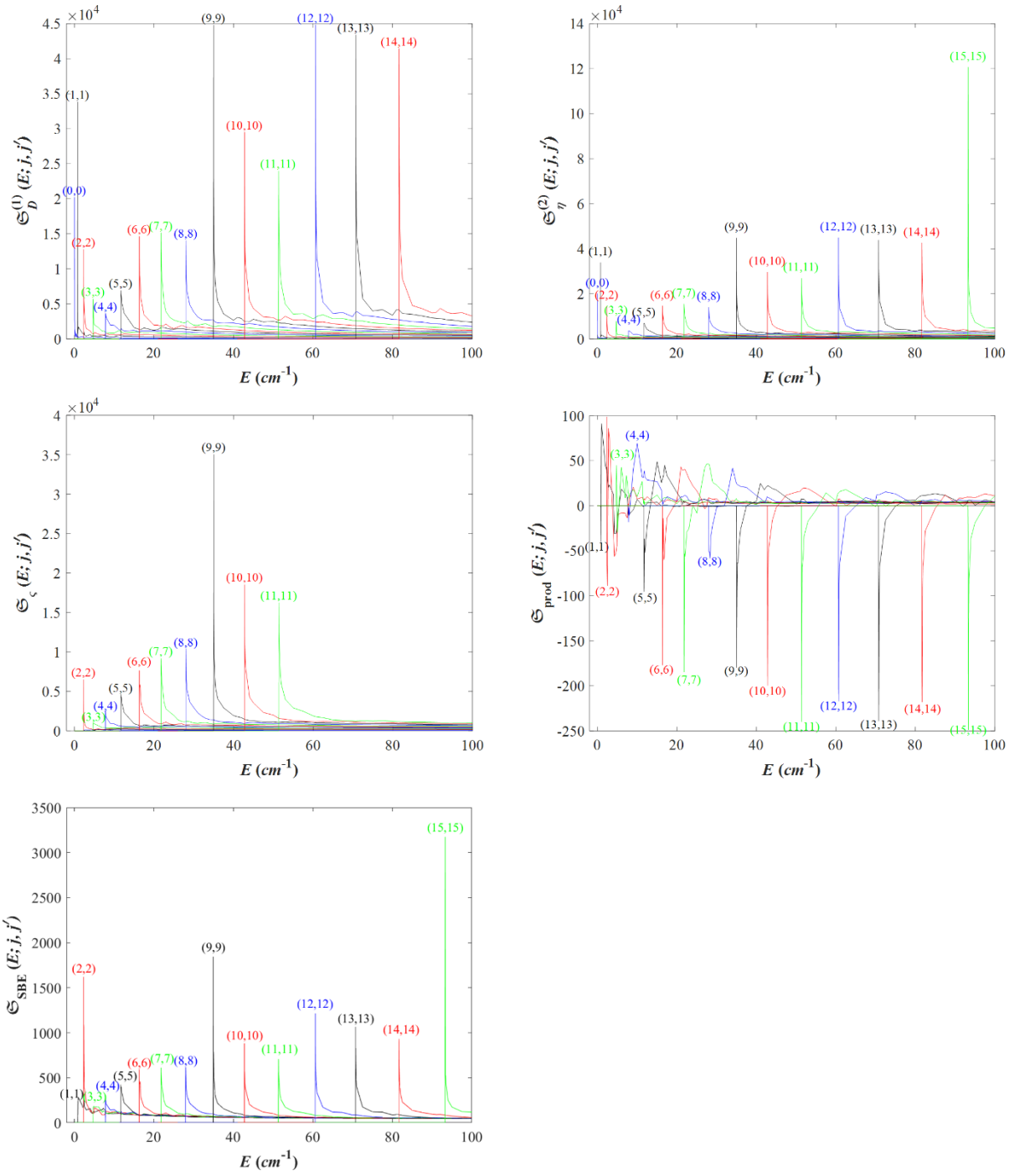

Fig. S.3. Energy dependent state-to-state cross sections ($\mathfrak{S}(E;j,j')$) as a function of energy (E) for diagonal transitions (i.e., j=j' in $j \rightarrow j'$).

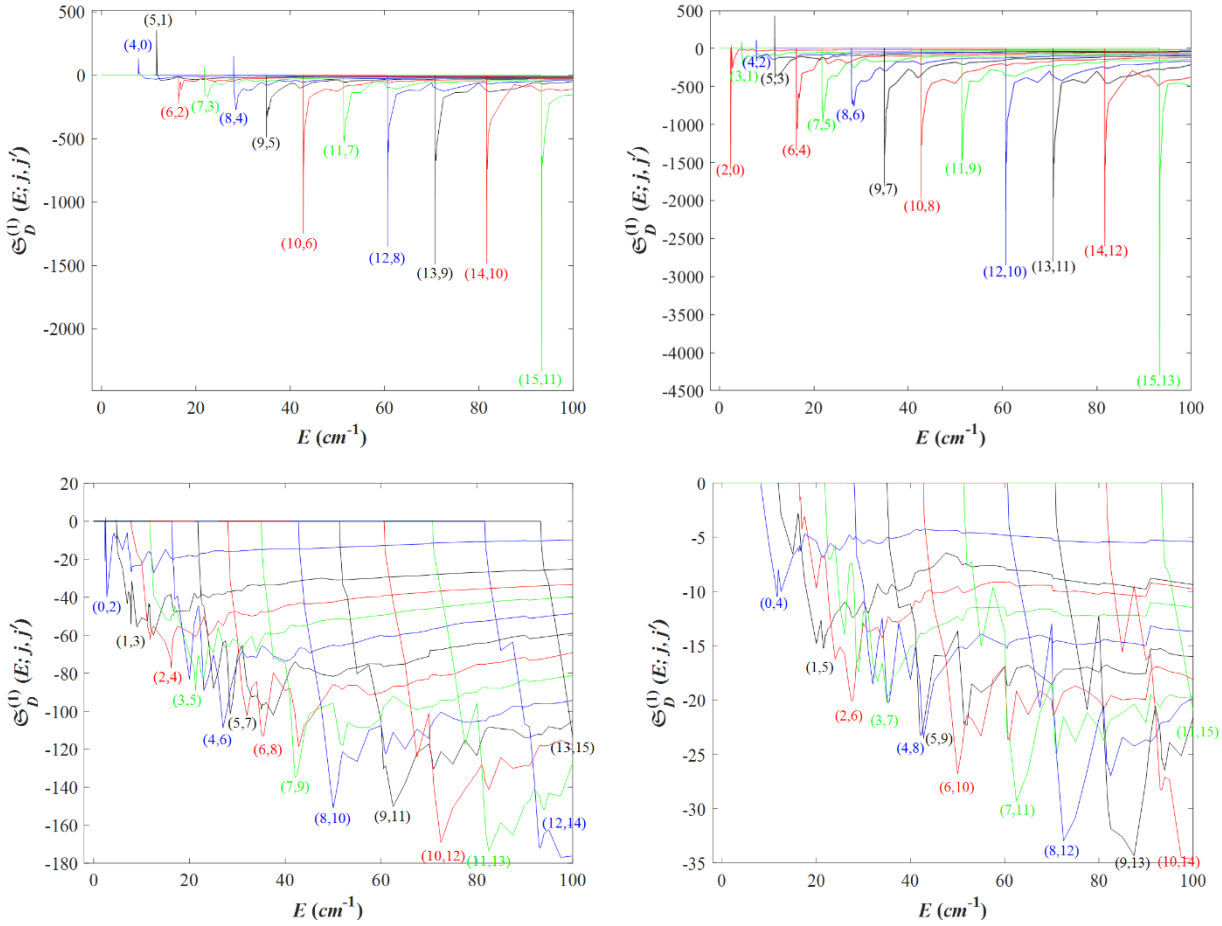

Fig. S.4. Energy dependent state-to-state diffusion coefficient cross section ($\mathfrak{S}_D^{(1)}(E;j,j')$) as a function of energy (E) for off-diagonal (i.e., $j \neq j'$ in $j \rightarrow j'$) rotational transitions.

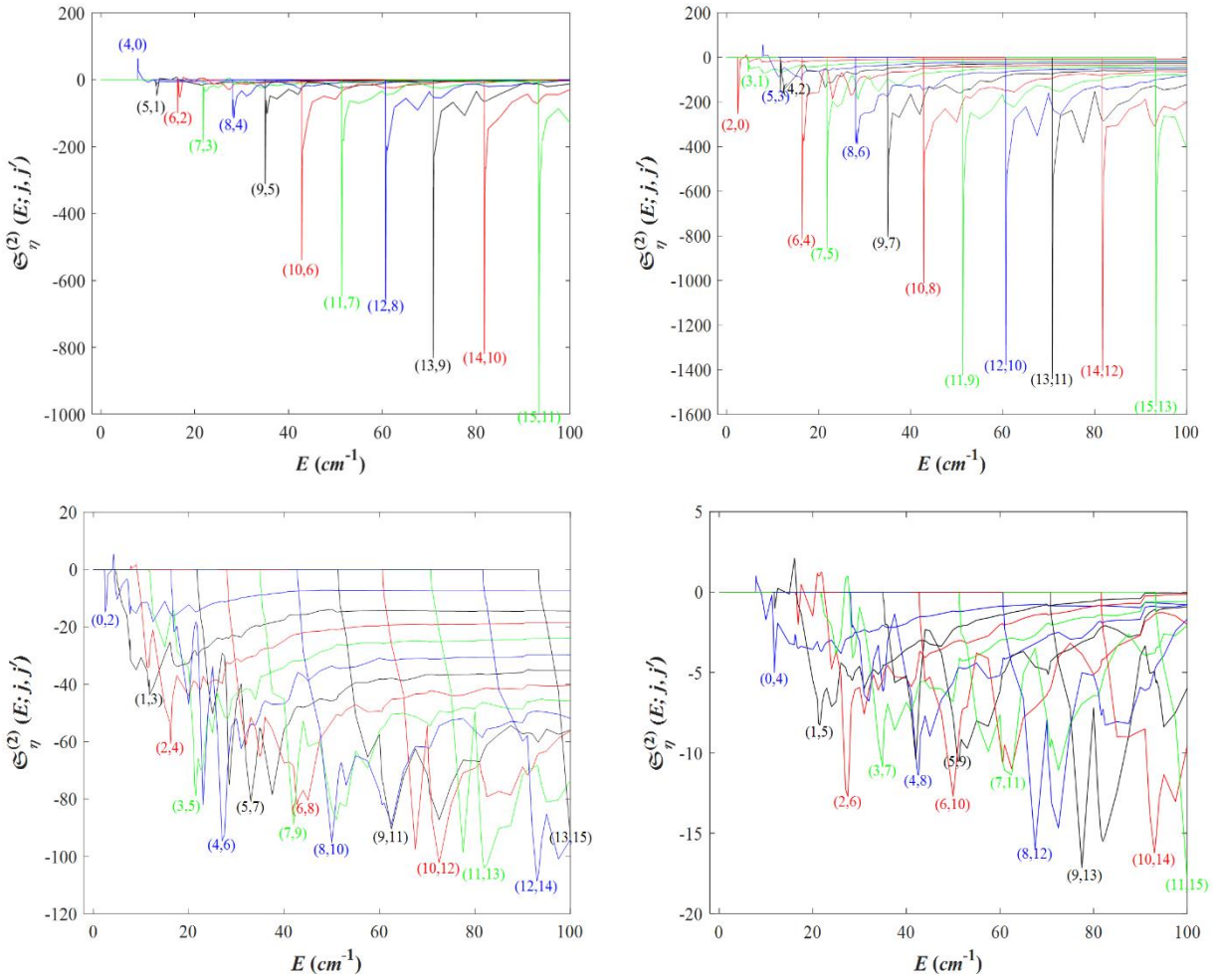

Fig. S.5. Energy dependent state-to-state viscosity coefficient cross section ($\mathfrak{S}_\eta^{(2)}(E;j,j')$) as a function of energy (E) for off-diagonal (i.e., $j \neq j'$ in $j \rightarrow j'$) rotational transitions.

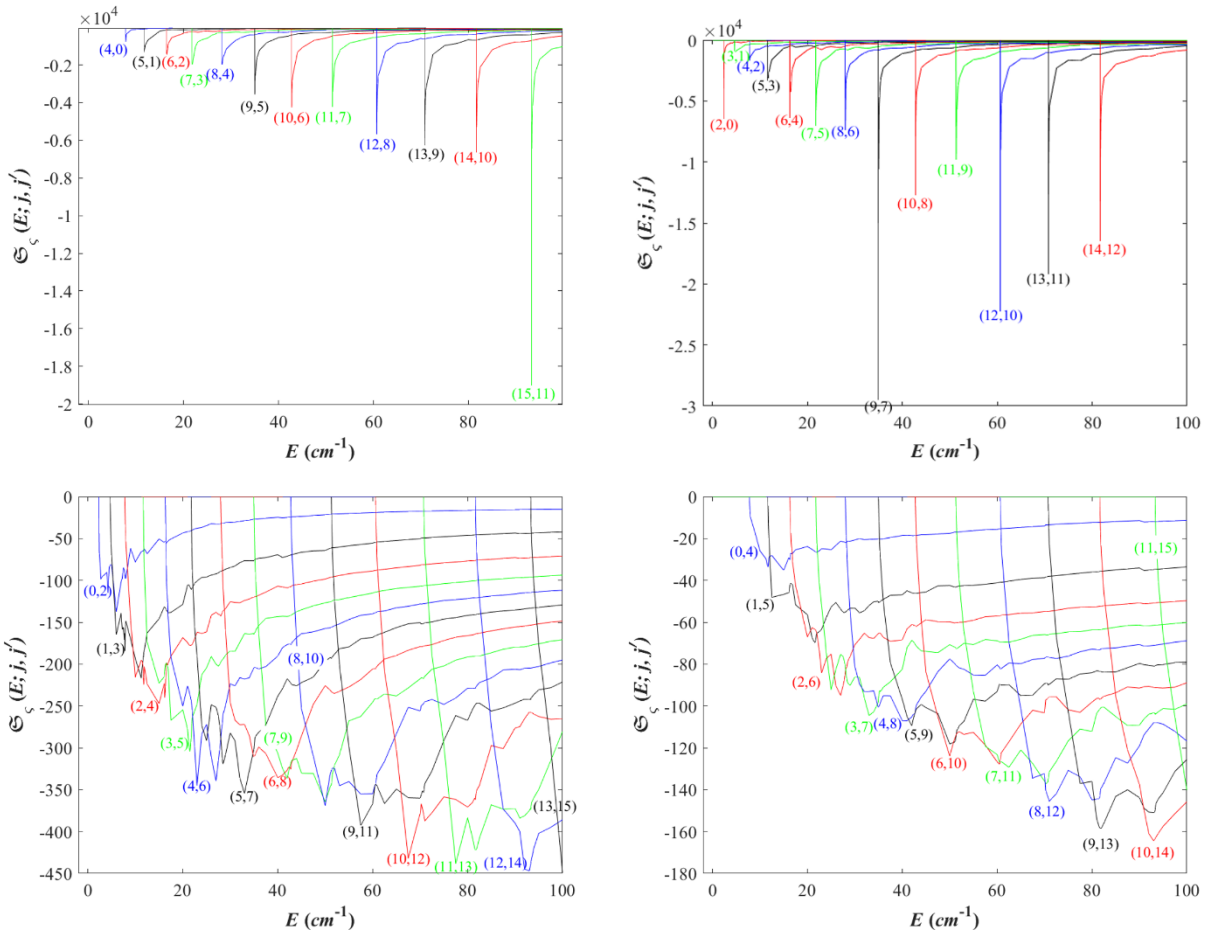

Fig. S.6. Energy dependent state-to-state rotational relaxation cross section ($\mathfrak{S}_{\varsigma}(E;j,j')$) as a function of energy (E) for off-diagonal (i.e., $j \neq j'$ in $j \rightarrow j'$) rotational transitions.

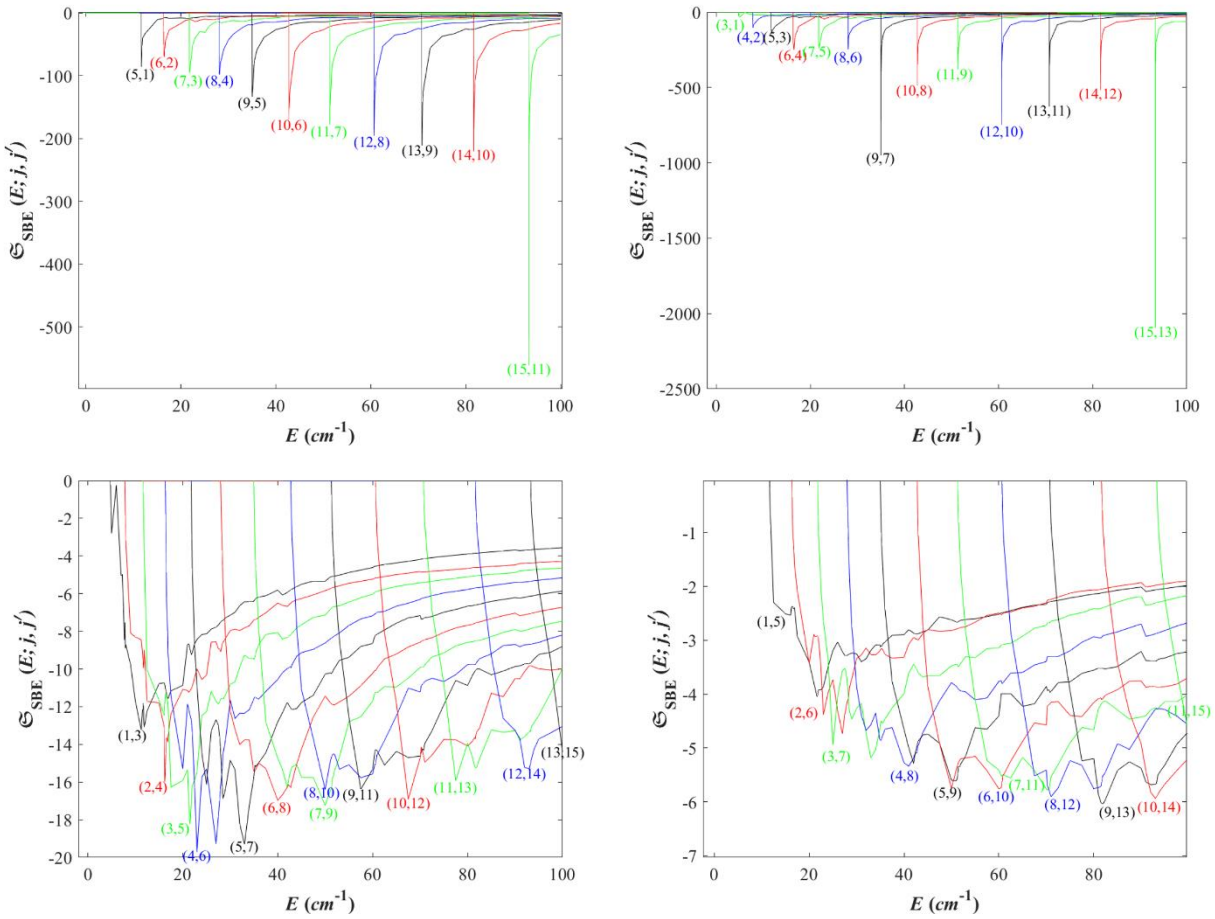

Fig. S.7. Energy dependent state-to-state viscomagnetic cross section ($\mathfrak{S}_{SBE}(E;j,j')$) as a function of energy (E) for off-diagonal (i.e., $j \neq j'$ in $j \rightarrow j'$) rotational transitions.

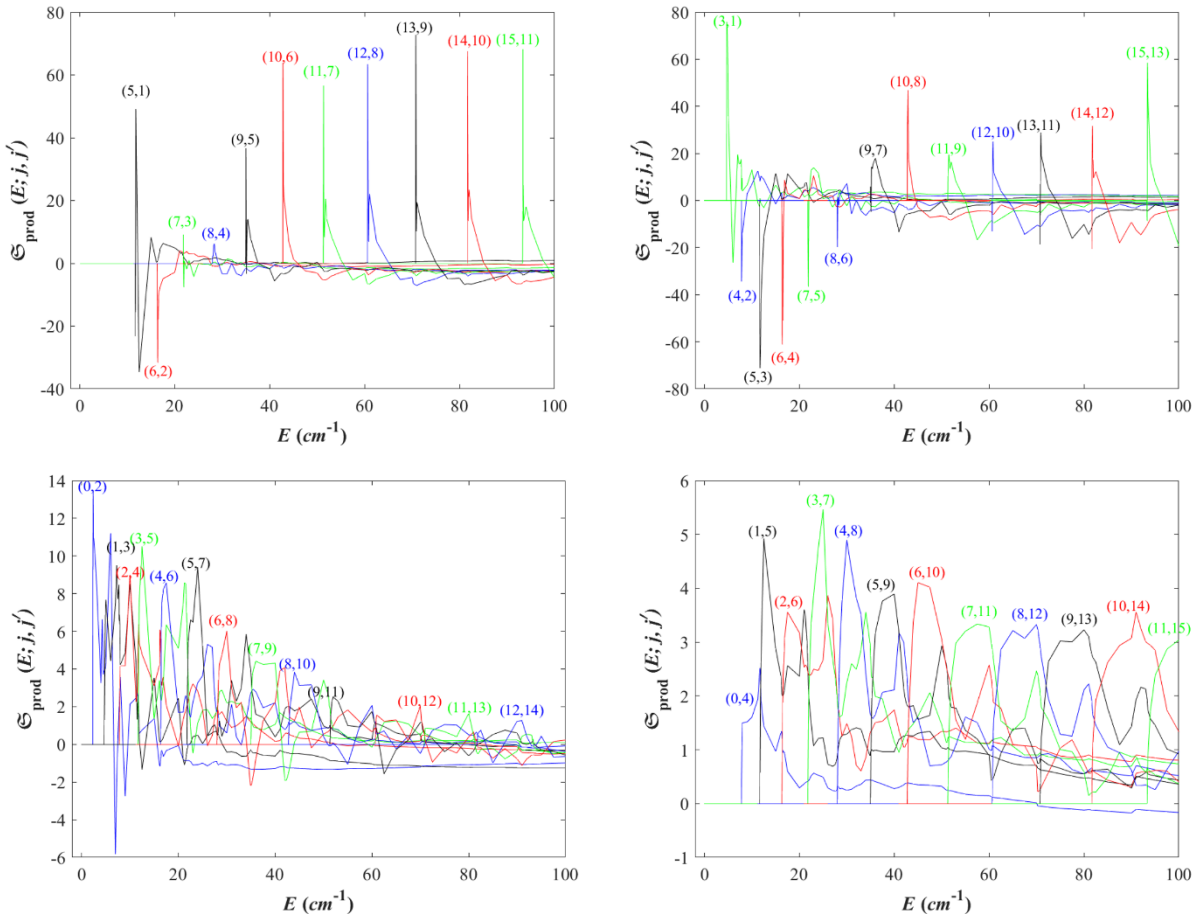

Fig. S.8. Energy dependent state-to-state production cross section ($\mathfrak{S}_{prod}(E;j,j')$) as a function of energy (E) for off-diagonal (i.e., $j \neq j'$ in $j \rightarrow j'$) rotational transitions.

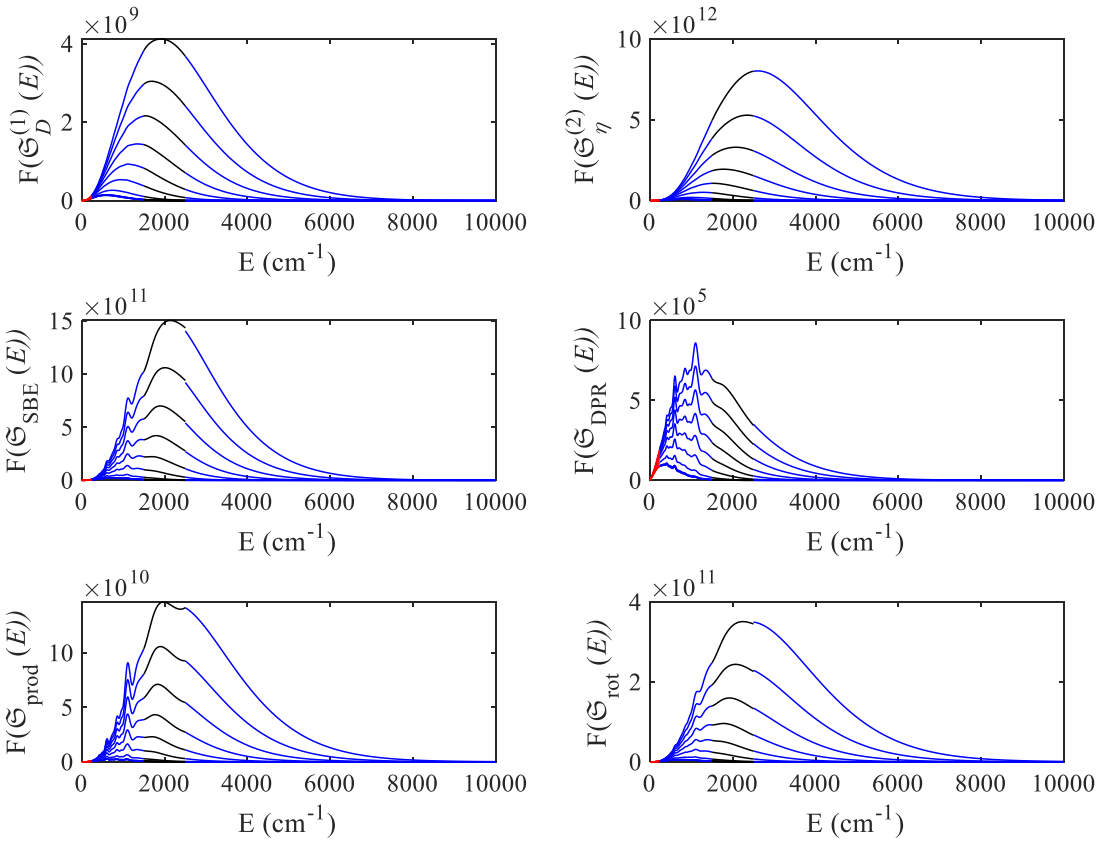

Fig. S.9. The integration function of the temperature dependent cross sections at different temperatures as function of energy. The lowest graph is at T = 20 K and the highest one corresponds to T = 1000 K in each figure.

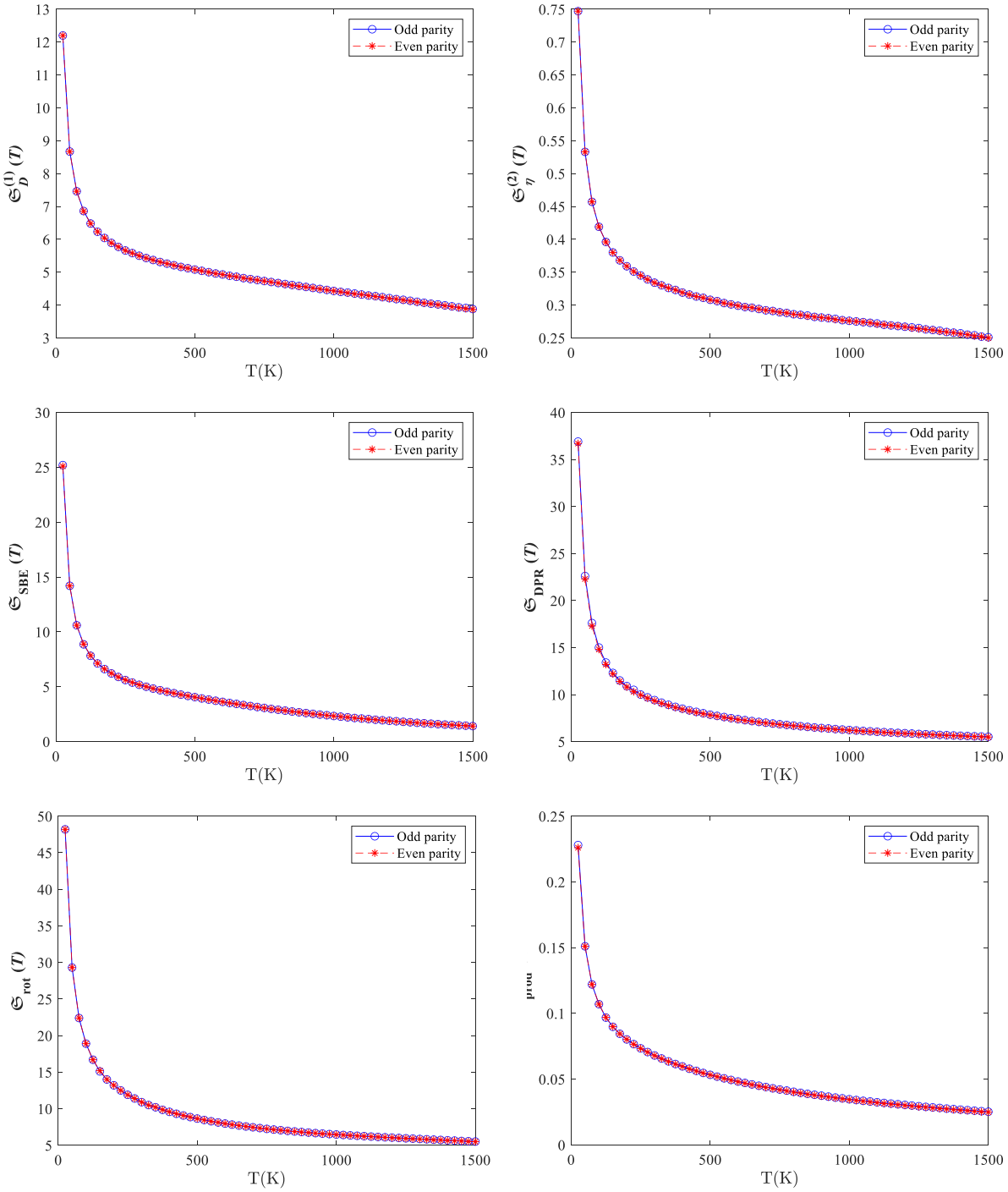

Fig. S.10. Temperature dependent SBE cross-sections ($\mathfrak{S}(T)$) for even ($j \rightarrow j'$; with j,j'=0, 2, 4, …) and odd ($j \rightarrow j'$; with j,j'=1, 3, 5, …) parities.

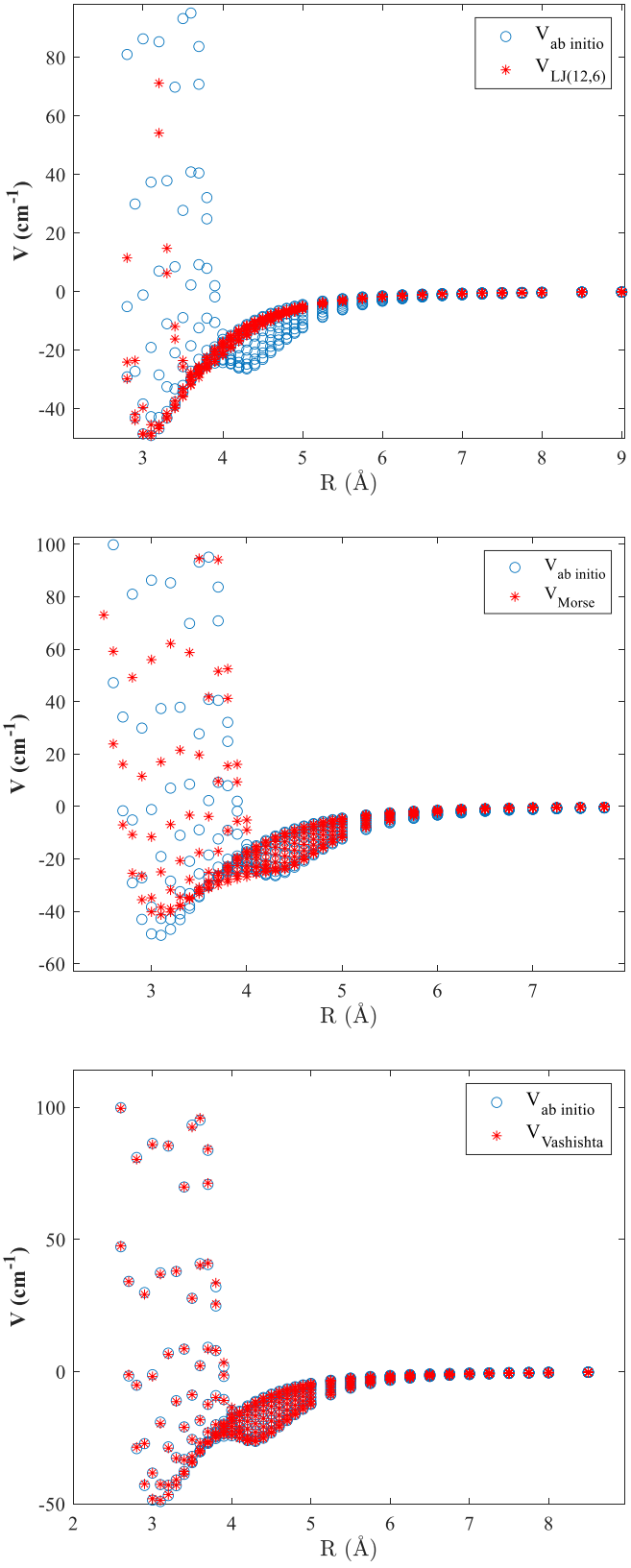

Fig. S.11. Comparison of the ab-initio potentials with LJ (12,6), Morse, and Vashishta potential models.

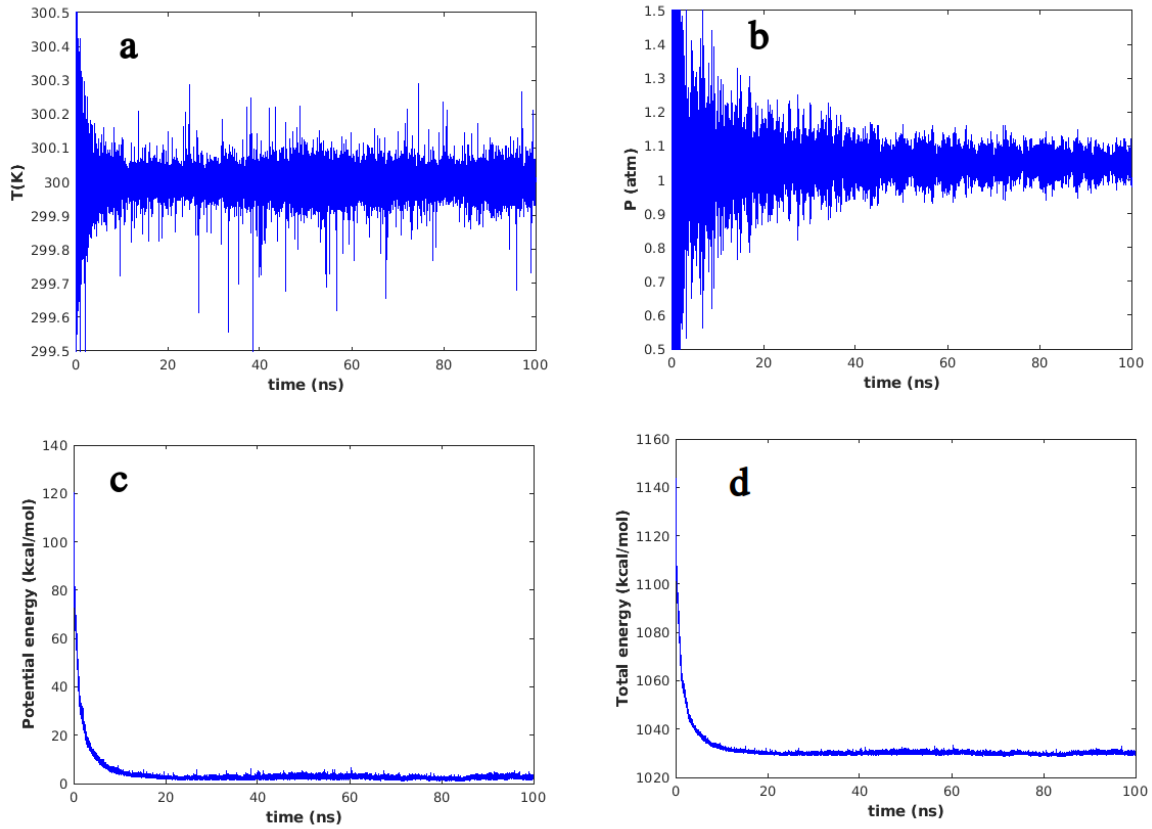

Fig. S.12 Calculated a: temperature, b: pressure, c: potential energy, and d: total energy as functions of simulation time for a 100 ns molecular dynamics simulation at T = 300 K using LJ (12,6) potential model.

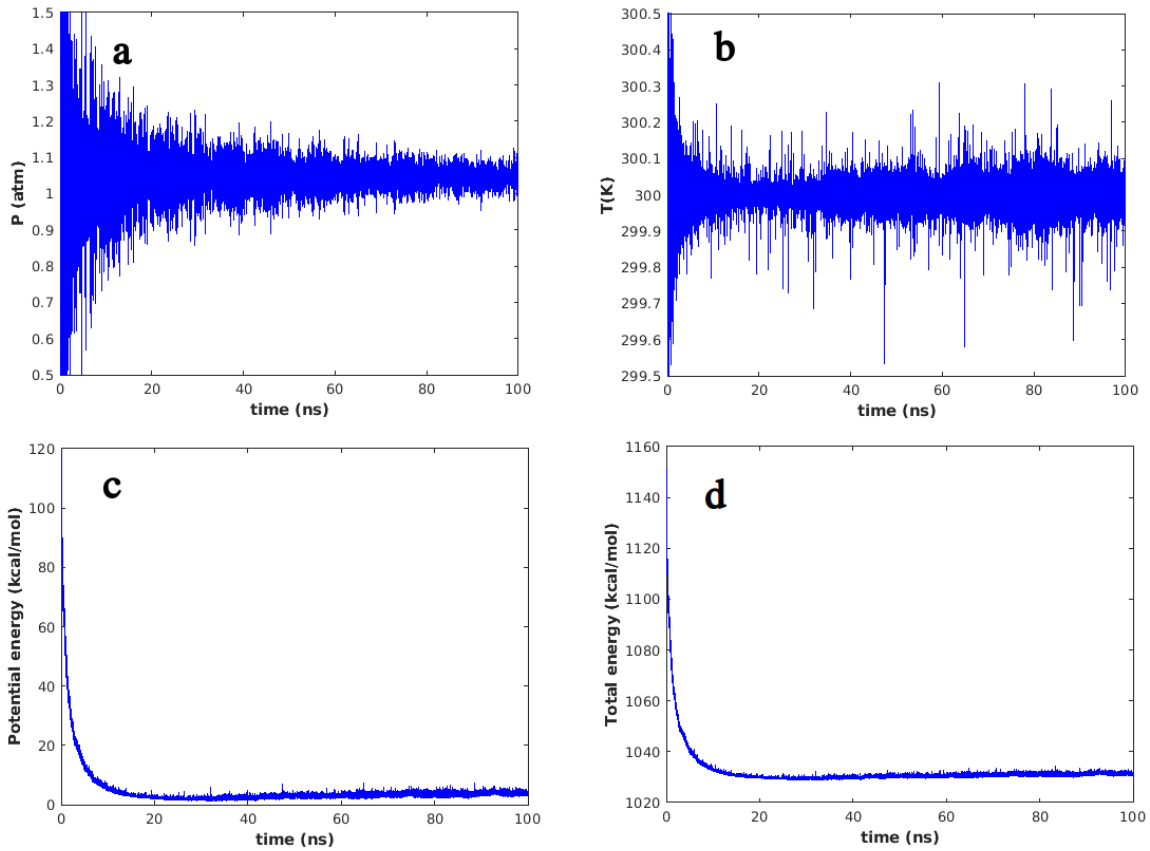

Fig. S.13. Calculated a: temperature, b: pressure, c: potential energy, and d: total energy as functions of simulation time for a 100 ns molecular dynamics simulation at T = 300 K using Morse potential model.

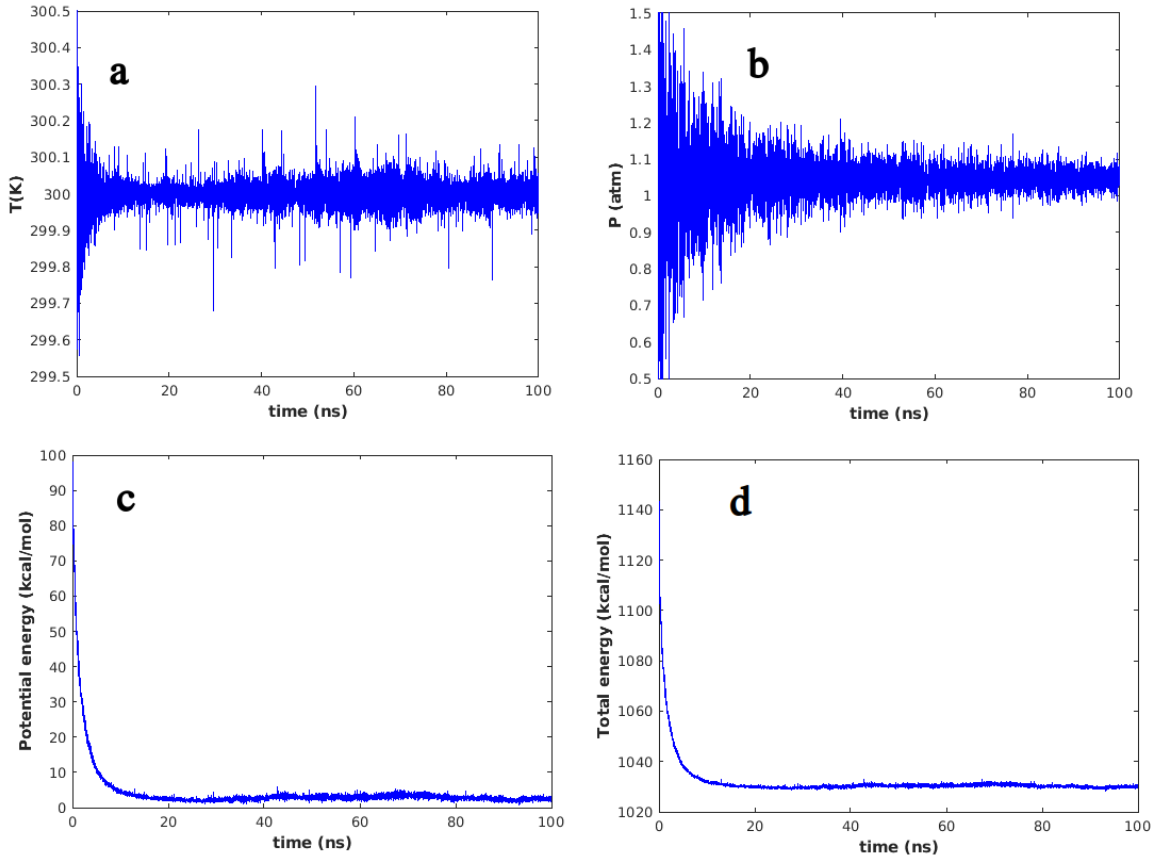

Fig. S.14. Calculated a: temperature, b: pressure, c: potential energy, and d: total energy as functions of simulation time for a 100 ns molecular dynamics simulation at T = 300 K using Vashishta potential model.

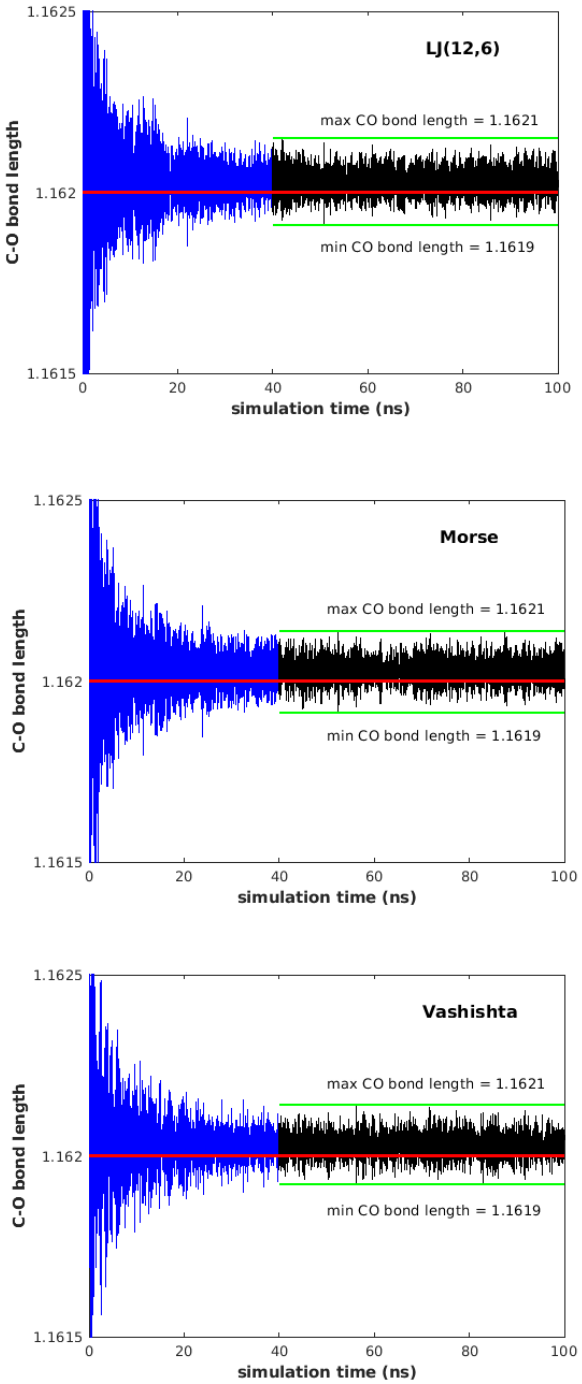

Fig. S.15. C-O bond length of CO_2 molecule during the molecular dynamic simulation at T = 300 K using different potential models.